

Densities mixture unfolding for data obtained from detectors with finite resolution and limited acceptance

N.D. Gagunashvili*,¹

University of Akureyri, Borgir, v/Nordurslód, IS-600 Akureyri, Iceland

Abstract

A procedure based on a Mixture Density Model for correcting experimental data for distortions due to finite resolution and limited detector acceptance is presented. Addressing the case that the solution is known to be non-negative, in the approach presented here, the true distribution is estimated by a weighted sum of probability density functions with positive weights and with the width of the densities acting as a regularisation parameter responsible for the smoothness of the result. To obtain better smoothing in less populated regions, the width parameter is chosen inversely proportional to the square root of the estimated density. Furthermore, the non-negative garrote method is used to find the most economic representation of the solution. Cross-validation is employed to determine the optimal values of the resolution and garrote parameters. The proposed approach is directly applicable to multidimensional problems. Numerical examples in one and two dimensions are presented to illustrate the procedure.

Key words: deconvolution, mixture densities, adaptive algorithm, inverse problem, single sided strongly varying spectra, regularisation

PACS: 02.30.Zz, 07.05.Kf, 07.05.Fb

*Tel.: +354-4608505; fax: +354-4608998

Email address: nikolai@unak.is (N.D. Gagunashvili)

¹Present address: Max-Planck-Institut für Kernphysik, PO Box 103980, 69029 Heidelberg, Germany

1. Introduction

The probability density function (PDF) $P(x')$ of an experimentally measured characteristic x' , in general, differs from the true physical PDF $p(x)$ because of the limited acceptance (probability) $A(x)$ to register an event with true characteristic x , finite resolution and bias in the response function $R(x'|x)$, which describes the probability to observe x' for a given true value x . Formally the relation between $P(x')$ and $p(x)$ is given by

$$P(x') \propto \int_{\Omega} p(x) A(x) R(x'|x) dx . \quad (1)$$

The integration in (1) is carried out over the domain Ω of the variable x . In practical applications the experimental distribution is usually discretised by using a histogram representation, obtained by integrating $P(x')$ over n finite sized bins

$$P_j = \int_{c_{j-1}}^{c_j} P(x') dx' \quad j = 1, \dots, n \quad (2)$$

with c_{j-1}, c_j the limits of bin j .

If a parametric (theoretical) model $p(x, a_1, a_2, \dots, a_l)$ for the true PDF is known, then the unfolding can be done by determining the parameters. For example, by a least squares fit to the binned data [1–3]. Here the model, which allows to describe the true distribution by a finite number of parameter values, constitutes a priori information which is needed to correct for the distortions by the experimental setup,

In contrast, model independent unfolding, as considered e.g. in [4–14], is an ill-posed problem, and every approach to solve it requires a priori information about the solution. Methods differ, directly or indirectly, in the way a priori information is incorporated in the result.

2. Description of the unfolding method

To solve the unfolding problem (1), a representation of the true distribution has to be chosen. This representation should be as flexible as possible and allow introducing a priori information. Classical kernel statistics is an example that approximates the true distribution by putting a $1/N$ -weighed copy of a kernel PDF at the location of each of N observed data points and adding them up (see e.g. [15]). With enough data, this comes arbitrarily close to any PDF. There exist methods that use a kernel representation of

the true distribution to solve also the inverse problem [16]. One drawback of this approach is that one has to store all the data points, another is that the known kernel based algorithms expect the response function of a set-up in analytical form, i.e. computer modelling cannot be used.

In this paper the use of a Mixture Density Model (MDM) [17, 19] to describe the true distribution $p(x)$ is proposed,

$$p(x) = \sum_{i=1}^s w_i K_i(x; a_{1i}, \dots, a_{li}), \quad (3)$$

where the $K_i(x; a_{1i}, \dots, a_{li})$ is the i th Probability Density Function in Mixture (PDFM) with parameters a_{1i}, \dots, a_{li} and the weight w_i the fraction of the i th PDFM.

The MDM lies between the cases of the parametric representation of the true density on one hand, i.e. the case when there is only one distribution in the sum (3), and the kernel statistics approach where the number of terms in the sum (3) is equal to the number of observations N . The MDM has a limited number of parameters for representing a PDF and computer modelling can be used to calculate the response of the system. The MDM is also convenient for taking into account different type of a priori information, such as knowledge about the type of distributions, constraints on parameters, smoothness of the distributions and so on. Ideas and achievements of regression analysis as well as classical kernel statistics can be used in applications of a MDM for estimating the densities.

Using Eq. (3) to parameterise the solution $p(x)$ reduces the unfolding problem from finding a solution in the infinite-dimensional space of all functions to finding a solution in a finite dimensional space. This way an approximation of the true density is performed which, in contrast to e.g. a discretisation by a histogram, has the advantage to introduce negligible quantisation errors for sufficiently smooth distributions.

Without loss of generality two-parametric PDFMs will be used throughout the paper. The first parameter, x_i , defines the mean value (location) of term i and the second one, λ_i , represents the standard deviation. Different smooth PDFMs commonly employed by kernel statistics, such as biweight, triweight, tricube, cosine, Cauchy, B-spline and other kernels can be used. Rather popular is the Gaussian Mixture Model (GMM) [18] with PDFMs

$$K_i(x; x_i, \lambda_i) = \frac{1}{\lambda_i \sqrt{2\pi}} \exp \left(-\frac{(x - x_i)^2}{2\lambda_i^2} \right), \quad (4)$$

which provides a rather flexible model in the approximation of a wide class of statistical distributions. The standard deviation λ_i acts as a regularisation parameter, which allows to adjust the smoothness of the result. Weights, positions x_i and standard deviations λ_i are determined by the unfolding procedure described below.

Substituting $p(x)$ as represented by Eq (3) into the basic Eq. (1) yields

$$P(x') = \sum_{i=1}^s w_i \int_{\Omega} K_i(x; x_i, \lambda_i) A(x) R(x'|x) dx , \quad (5)$$

and taking statistical fluctuations into account, the relation between the weights w_i and the histogram of the observed distribution becomes a set of linear equations

$$\mathbf{P} = \mathbf{Q}\mathbf{w} + \boldsymbol{\epsilon} , \quad (6)$$

where \mathbf{P} is the n -component column vector of the experimentally measured histogram, $\mathbf{w} = (w_1, w_2, \dots, w_s)^t$ is the s -component vector of weights and \mathbf{Q} is an $n \times s$ matrix with elements

$$Q_{ji} = \int_{c_{j-1}}^{c_j} K_i(x; x_i, \lambda_i) A(x) R(x'|x) dx \quad j = 1, \dots, n; \quad i = 1, \dots, s . \quad (7)$$

The vector $\boldsymbol{\epsilon}$ is an n -component vector of random deviates with expectation value $E[\boldsymbol{\epsilon}] = \mathbf{0}$ and covariance matrix \mathbf{C} , the diagonal elements of which being $\text{Var}[\boldsymbol{\epsilon}] = \text{diag}(\sigma_1^2, \sigma_2^2, \dots, \sigma_n^2)$, where σ_j is the statistical error of the measured distribution for the j th bin. Each column of the matrix \mathbf{Q} is the response of the system to one of the PDFM in the mixture model for the true distribution. Numerically the calculation of the column vectors can be done by weighting events of a Monte Carlo sample such that they follow the corresponding PDFM, see Ref. [20], and taking the histogram of the observed distribution obtained with the weighted entries.

By a non-negative least-squares fit, the weight vector \mathbf{w} in Eq. (6) for a given set of PDFMs is determined such that it minimizes

$$X^2 = (\mathbf{P} - \mathbf{Q}\hat{\mathbf{w}})^t \mathbf{C}^{-1} (\mathbf{P} - \mathbf{Q}\hat{\mathbf{w}}) \quad (8)$$

under the constraints

$$w_i \geq 0 \quad i = 1, \dots, s . \quad (9)$$

Following reference [21], if an unconstrained solution satisfies Eq. (9) then $\hat{\mathbf{w}}$ solves the constrained problem. Otherwise, the solution to the constrained

problem must be a boundary point of $[0, +\infty)^s$ and therefore at least one $w_i = 0$. It follows that after performing all possible regressions with one or more w_i in Eq.(9) set to zero, the non-negative problem is solved by picking the subset of w_i satisfying Eq.(9) such that X^2 as defined in Eq.(8) is smallest. The numerical algorithm and computer program for solving this minimisation problem has been developed in references [21, 22]. Here, first the subset of components equal to zero is determined iteratively, and the vector of the remaining indices $\hat{\mathbf{w}}$ is found by simple linear regression

$$\hat{\mathbf{w}} = (\mathbf{Q}^t \mathbf{C}^{-1} \mathbf{Q})^{-1} (\mathbf{Q}^t \mathbf{C}^{-1}) \mathbf{P}, \quad (10)$$

where \mathbf{Q} is the submatrix of \mathbf{Q} that corresponds to the subset of indices of positive components of the solution. The result of the fit is an estimate of the unfolded distribution $\hat{p}(x)$, defined by a subset of parameters $x_i, \lambda_i, i = 1, \dots, k$ which are summed with positive weights $\hat{w}_i, i = 1, \dots, k$ to yield

$$\hat{p}(x) = \sum_{i=1}^k \hat{w}_i K_i(x; x_i, \lambda_i). \quad (11)$$

The choices of the optimal type of PDFMs and the values of parameters (mean values and the standard deviations for the GMM model) are driven by the accuracy and the complexity of the model. The goal is a simple, and at the same time, accurate solution of the problem. A figure of merit for the accuracy is the Prediction Error (PE) [23], defined as the expectation value of the average squared normalised residual when using the predictor $\mathbf{Q}\hat{\mathbf{w}}$ to describe an independent experimentally measured histogram \mathbf{P}^{new} drawn from the same parent distribution as the original,

$$PE(\mathbf{Q}\hat{\mathbf{w}}) = E\left[\frac{1}{n}(\mathbf{P}^{new} - \mathbf{Q}\hat{\mathbf{w}})^t \mathbf{C}^{-1}(\mathbf{P}^{new} - \mathbf{Q}\hat{\mathbf{w}})\right]. \quad (12)$$

The expectation is taken over \mathbf{P}^{new} . In the following we will denote the predictor $\mathbf{Q}\hat{\mathbf{w}}$ as $\hat{\mathbf{P}}$ and call it the fitting histogram.

Following reference [23], V -fold Cross-Validation allows to estimate $PE(\mathbf{Q}\hat{\mathbf{w}})$. Here the given data set \mathcal{U} is split into V subsets $\mathcal{U}_1, \dots, \mathcal{U}_V$ with equal number of events. The complementary sets are denoted by $\mathcal{U}^{(v)} = \mathcal{U} - \mathcal{U}_v$. Applying the minimisation procedure to $\mathcal{U}^{(v)}$ and forming the predictors $\mathbf{Q}\hat{\mathbf{w}}^{(v)}$, the Cross-Validation error (CV) is defined by

$$CV = \frac{1}{n} \sum_{v=1}^V (\mathbf{P}_v - \mathbf{Q}\hat{\mathbf{w}}^{(v)})^t \mathbf{C}^{-1}(\mathbf{P}_v - \mathbf{Q}\hat{\mathbf{w}}^{(v)}), \quad (13)$$

where \mathbf{P}_v is the vector of histogram contents for the subset of the data \mathcal{U}_v . The Cross-Validation error is the estimate of the Prediction Error

$$CV = \widehat{PE}(\mathbf{Q}\hat{\mathbf{w}}) . \quad (14)$$

In order to have sufficient sampling of the configuration space, the number of folders used in the Cross-Validation procedure should not be too small. On the other hand, for statistically meaningful results, it should not be too large either. Practice shows that taking V in the range between 5 and 10 usually gives satisfactory results, and that the performance is not sensitive to the exact choice.

The proposed unfolding procedure consists of three steps:

2.1. First step

The positions $\{x_i\}$ of the PDFMs are drawn randomly from a uniform distribution on the allowed range of x and with a number of PDFMs such that the average distance between individual centers is significantly smaller than the width of the PDFMs.

In order to minimise the loss of information due to binning, the number of bins for the measured histogram \mathbf{P} should be as large as possible. On the other hand, in order to have meaningful error estimates for the least squares fits that determine $\hat{\mathbf{w}}$, the number of entries in a single bin should not be less than 25. Binning with approximately equal number of events in each bin is preferable.

In this first step the width for all PDFMs in the mixture is taken to be the same, $\lambda_i = \lambda$. Different values λ are tried and the $\hat{\lambda}$ with the smallest Cross-Validation error

$$\hat{\lambda} = \underset{\lambda}{\operatorname{argmin}} CV(\lambda) \quad (15)$$

is selected.

2.2. Second step

Exploiting the information gained so far, the procedure is repeated with positions $\{x_i\}$ of the PDFMs randomly drawn according to the estimate of the true density $\hat{p}(x)$ (11) obtained in the first step. In addition, the widths

of the PDFMs $\{\hat{\lambda}_i\}$ are taken to be inversely proportional to the square root of the result from the first step at the position $\{x_i\}$

$$\hat{\lambda}_i = \frac{\hat{\lambda}}{\sqrt{\hat{p}(x_i)}} \quad (16)$$

with the value of $\hat{\lambda}$ again determined by means of Cross-Validation. This second step is motivated by the results of reference [24], where it is shown that by this way the bias of a kernel estimation of a PDF can be decreased. The approach balances better smoothing in less densely populated regions against the possibility to resolve finer structures in regions with a higher sampling. It is plausible that for the unfolding case the bias on the shape of the density estimate will decrease also. Finally it has to be noted that this second step can be iterated several times, even though practical examples show that the gain is small.

It is recommended to use the same number of PDFMs for the second step as in the first step or more.

2.3. Third step

Since the number of terms obtained by the previous two steps can still be large, with not all PDFMs contributing independent information, a third step is added to select the most relevant subset. To reduce the number of the PDFMs, the non-negative garrote method [23] is used. It amounts to taking the set of non-zero weights $\{\hat{w}_j\}$ obtained in the second step and finding coefficients $\{c_j\}$ that minimise

$$\sum_{i=1}^n (P_i - \sum_{j=1}^s Q_{ij} c_j \hat{w}_j)^2 / \sigma_i^2 \quad (17)$$

under the constraints

$$c_j \geq 0 \quad \text{and} \quad \sum_{j=1}^s c_j \leq r . \quad (18)$$

For $r \geq \sum \hat{w}_i$ the solution from the previous step is not touched. For smaller values the garrote eliminates some of weights and modifies others, such that $\tilde{w}_j(r) = c_j \hat{w}_j$ are the new values of the weights for the PDFMs of the estimate the unfolded distribution. Cross-validation is used to choose the optimal garrote parameter r . To reduce a potential bias introduced by the garrote, the weights of the PDFMs are again determined by a non-negative least squares fit on the remaining terms.

2.4. Quality assessment and error propagation

The quality of the fit can be assessed with common tools used in regression analysis [25]:

1. p -value of the fit is defined by $Pr(X \geq \sum_{i=1}^n (P_i - \hat{P}_i)^2 / \sigma_i^2) | \chi_{n-s}^2$, where Pr stands for probability
2. analysis of the normalised residuals $Res_i = (P_i - \hat{P}_i) / \sigma_i, i = 1, \dots, n$
 - (a) as a function of the estimated value $\hat{\mathbf{P}}$
 - (b) as a function of the observed value x'
3. Q-Q plot: $(data\ quantile)_i = (\text{number of residuals} \leq Res_i) / n$ versus $(theoretical\ quantile)_i = Pr(X \leq (Res_i | \mathcal{N}(0, 1))), i = 1, \dots, n$

Since the unfolding procedure described above is not analytically defined, the bootstrap approach [26] is the method of choice to estimate the statistical uncertainties of the unfolding result. Keeping the normalisation of the observed histogram constant, replications are generated according to the multinomial distribution

$$\frac{N!}{N_1! N_2! \dots N_n!} \mathcal{P}_1^{N_1} \dots \mathcal{P}_n^{N_n} \quad \text{with} \quad \mathcal{P}_i = \frac{\sum_{j=1}^s Q_{ij} \hat{w}_j}{\sum_{i=1}^n \sum_{j=1}^s Q_{ij} \hat{w}_j}, \quad (19)$$

where the set of positive weights obtained in the final step is used.

A histogram representation $\hat{\mathbf{p}}$ for the unfolded distribution $\hat{p}(x)$ with m bins integrating over the x -intervals $[b_{i-1}, b_i], i = 1, \dots, m$ is obtained by

$$\hat{\mathbf{p}} = \mathbf{K} \hat{\mathbf{w}}, \quad (20)$$

where \mathbf{K} is an $m \times k$ matrix with elements

$$K_{ij} = \int_{b_{i-1}}^{b_i} K_j(x; x_j, \lambda_j) dx. \quad (21)$$

The unfolding method described above assumes that the matrix \mathbf{Q} relating the weight vector $\hat{\mathbf{w}}$ to the measurements \mathbf{P} is known exactly. Therefore, when \mathbf{Q} is determined by means of a Monte Carlo simulation, the Monte Carlo sample should be significantly larger than the data sample.

In an extension of the method which is applicable also in cases where the Monte Carlo statistics is of the same order or less than the data statistics is obtained by using a modified matrix of errors \mathbf{C} which includes statistical errors for the elements of matrix \mathbf{Q} [27], and the Cross-Validation statistics substituted by the goodness-of-fit statistics for the comparing unweighted \mathbf{P}_v and weighted $\mathbf{Q} \hat{\mathbf{w}}^{(v)}$ histograms given in references [28, 29].

3. Numerical examples

Three types of numerical examples are discussed to illustrate the unfolding procedure. The first is the classic example of a double peak structure proposed by V. Blobel [5]. The second is a strongly varying one-sided distribution, and the third one a two-dimensional case.

3.1. Double peak structure

The method described above is illustrated using the example proposed in reference [5]. The true distribution, defined on the range $x \in [0, 2]$ is described by a sum of three Breit-Wigner functions

$$p(x) \propto \frac{4}{(x - 0.4)^2 + 4} + \frac{0.4}{(x - 0.8)^2 + 0.04} + \frac{0.2}{(x - 1.5)^2 + 0.04} \quad (22)$$

from which the experimentally measured distribution is obtained by

$$P(x') \propto \int_0^2 p(x) A(x) R(x'|x) dx, \quad (23)$$

with an acceptance function $A(x)$

$$A(x) = 1 - \frac{(x - 1)^2}{2} \quad (24)$$

and a response function describing a biased measurement with gaussian smearing

$$R(x'|x) = \frac{1}{\sqrt{2\pi}\sigma} \exp\left(-\frac{(x' - x + 0.05x^2)^2}{2\sigma^2}\right) \quad \text{with } \sigma = 0.1. \quad (25)$$

The acceptance and resolution functions are shown in Fig. 1. Also shown is an example for the measured distribution obtained by simulating a sample of $N = 5\,000$ events. A histogram with number of bins $n = 87$ and

approximately equal number of events in each bin was used.

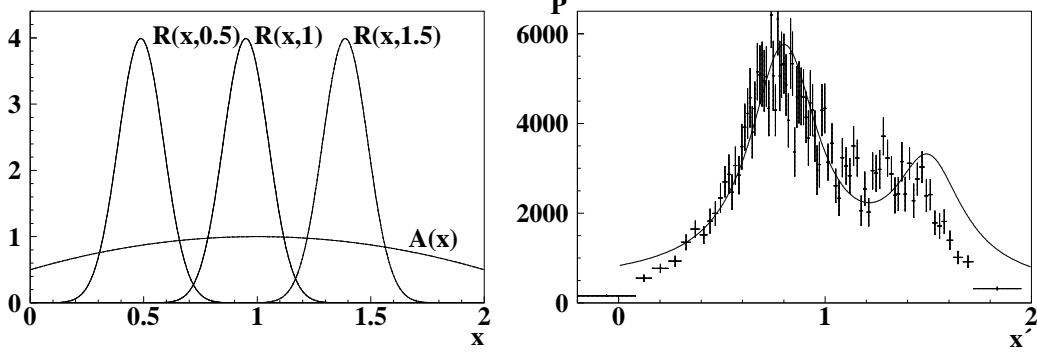


Figure 1: Acceptance function $A(x)$ and resolution function $R(x'|x)$ for $x = 0.5, 1.0$ and 1.5 (left) and histogram of the measured distribution \mathbf{P} based on a sample of 5 000 events generated for the true distribution (right). The bin contents of the histogram are normalised to the bin width. The true distribution $p(x)$ is shown by the curve (right).

The PDFMs were defined in the form

$$K_i(x; x_i, \lambda_i) \propto \left[\frac{1}{\lambda_i \sqrt{2\pi}} \exp\left(-\frac{(x - x_i)^2}{2\lambda_i^2}\right) + \frac{1}{\lambda_i \sqrt{2\pi}} \exp\left(-\frac{(x + x_i)^2}{2\lambda_i^2}\right) + \frac{1}{\lambda_i \sqrt{2\pi}} \exp\left(-\frac{(x - 4 + x_i)^2}{2\lambda_i^2}\right) \right] I_{\{x \in [0;2]\}},$$

with the indicator function

$$I_{\{\dots\}} = \begin{cases} 1 & \text{if the condition given in the curly brackets is satisfied} \\ 0 & \text{otherwise} \end{cases}.$$

The functional form is chosen in accordance with the recommendation formulated in reference [15] for PDFs defined on the restricted interval. An initial set of 400 PDFMs was used with positions x_i uniformly distributed over the interval $[0, 2]$. For the determination of the matrix \mathbf{Q} a sample of 500 000 Monte Carlo events was simulated. Here a uniform true distribution was taken and the responses of the individual PDFMs were calculated by weighting the Monte Carlo events with weights proportional to the value of

the respective PDFM [20].

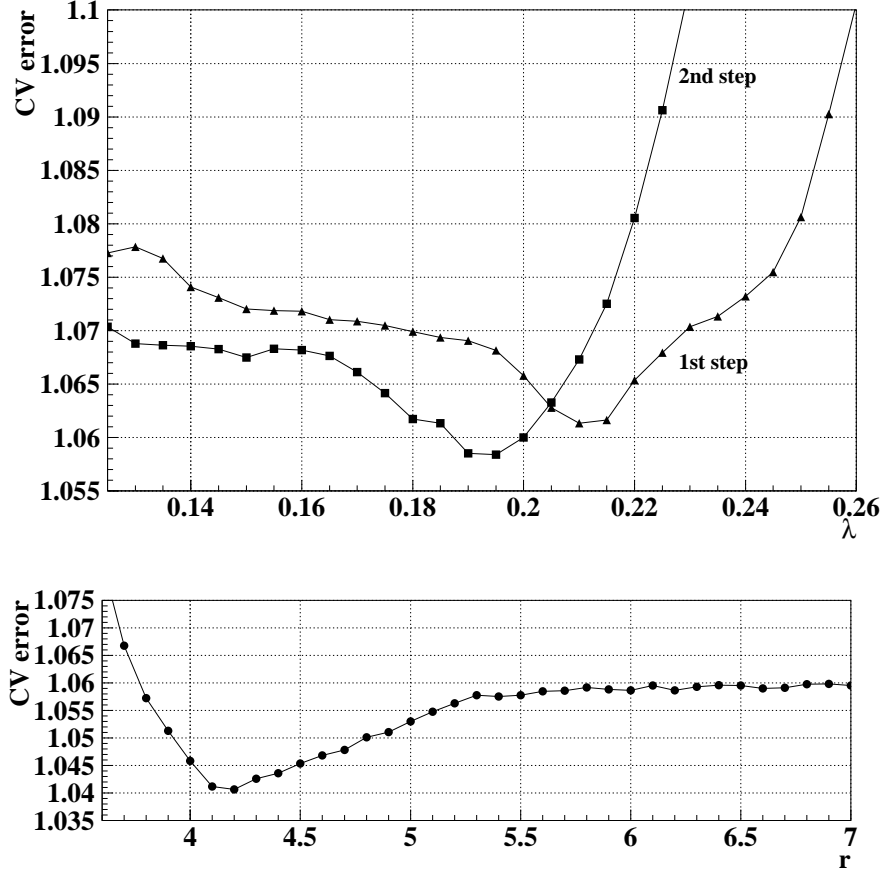


Figure 2: Cross-Validation errors of the first and second unfolding step as a function of λ (top), and Cross-Validation error in the third step for $\hat{\lambda} = 0.19$ as a function of the garrote parameter r (bottom).

The top plot of Fig.2 shows how the Cross-Validation error for 5-fold Cross-Validation in the first and the second step behaves as a function of λ . One observes that the best value in the second step is slightly smaller in step 2, and also that the Cross-Validation error is reduced. This shows that adapting the widths of the PDFMs in the model according to the estimated density not only provides better smoothing in regions of small statistics, but also improves the quality of the unfolding result. The best value is found as $\hat{\lambda} = 0.19$. This value is used in the third step, where the non-negative garrote is employed to reduce the number of the PDFMs. The bottom frame of Fig.2

shows the Cross-Validation error as a function of the garrote parameter r . Again a significant improvement is found for $r = 4.2$. For the statistics used in this example, the final estimate of the true distribution contains only three terms.

The quality of the unfolding result is illustrated by Fig. 3. It shows how the folded estimate of true distribution \hat{P} , with three components, approximates the measured distribution, together with plots of the residuals and the quantile-quantile plot. No structure in either of the control plots is observed. The p -value from the test comparing the histogram of the measured distribution P and the fitting histogram \hat{P} is $p = 0.6$.

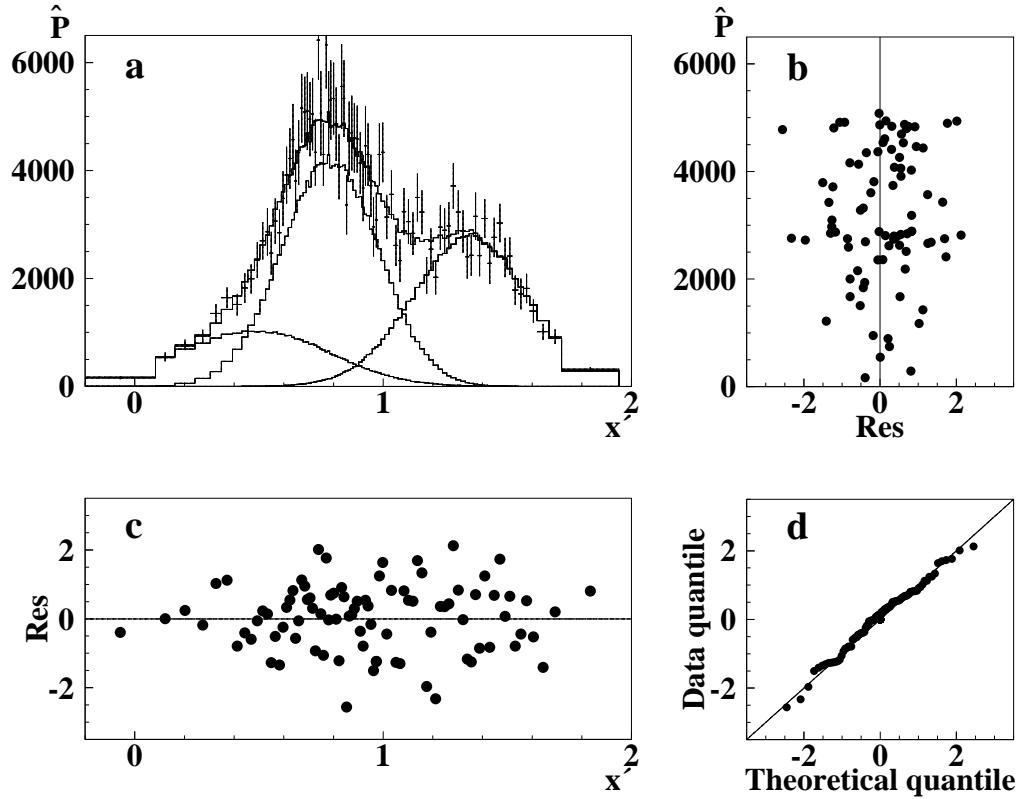


Figure 3: Illustration of the quality of the unfolding result. (a) folded estimate of the true distribution \hat{P} (solid histogram), with tree components, compared to the measured distribution P ; (b) normalised residuals of the fit as a function of \hat{P} ; (c) normalized residuals as a function of x' ; (d) quantile-quantile plot for the normalized residuals.

The estimate of the true distribution obtained by the unfolding proce-

ture is presented in Figs. 4 and 5. The components of the unfolding results together with the estimate $\hat{p}(x)$ in Fig. 4. Also shown are the two standard deviation bands $\pm 2\delta(x)$ compared to the true distribution $p(x)$. Histogram presentations of the unfolded distribution are shown in Fig. 5 for $n = 12$ bins as in reference [5] and for $n = 40$ bins as in reference [9]. Standard deviation bands and bin-by-bin uncertainties for the histograms were estimated by the bootstrap method.

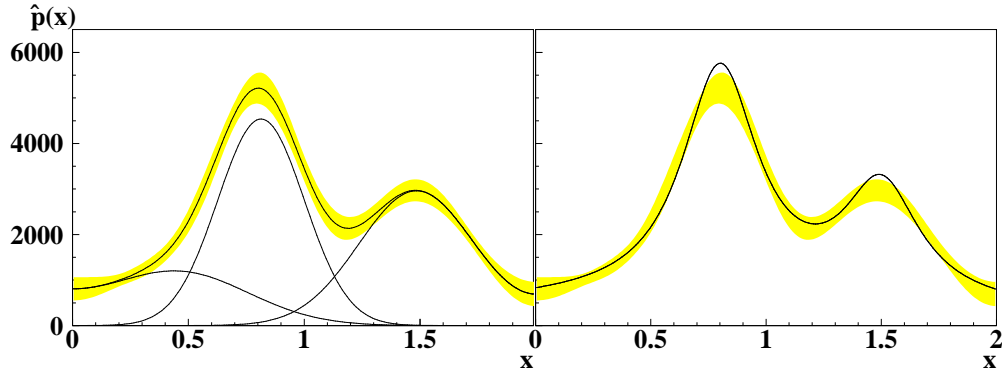


Figure 4: Components of the unfolded distribution and the unfolded distribution $\hat{p}(x)$ given by the sum of the components with $\pm 2\delta(x)$ interval (left) and the two standard deviation band overlaid with the true distribution $p(x)$ (right).

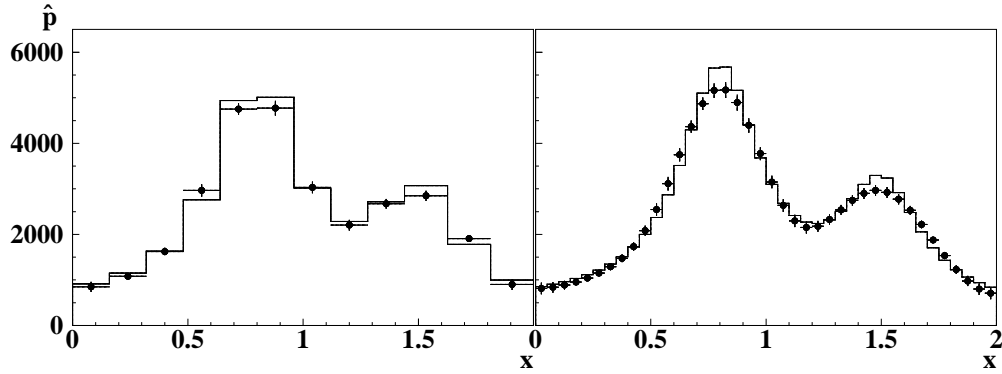


Figure 5: Binned representation of the unfolding result \hat{p}_i for $n = 12$ (left) and $n = 40$ (right) bins. The points with error bars are the estimate obtained by the unfolding procedure, the histogram shows the true bin contents p_i .

For the illustration of the proposed algorithm, the unfolded distributions

for steps 1 and 2 on Fig. 6 are presented as well as Table 1 with values of parameters x_i , $\hat{\lambda}_i$, \hat{w}_i of the components for the three steps of the procedure.

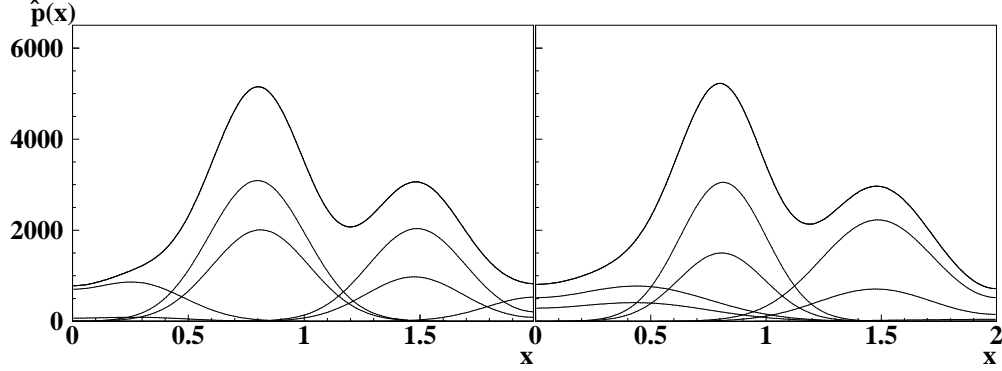


Figure 6: Components of the unfolded distribution and the unfolded distribution $\hat{p}(x)$ given by the sum of the components for the step 1 (left) and for the step 2 (right).

Table 1: Values of parameters x_i , $\hat{\lambda}_i$, \hat{w}_i of the PDFMs represented unfolded distributions for three steps of procedure

i	1	2	3	4	5	6	7	
x_i	0.275	1.475	1.992	1.487	0.798	0.812	0.284	Step 1
$\hat{\lambda}_i$	0.210	0.210	0.210	0.210	0.210	0.210	0.210	
\hat{w}_i	0.087	0.103	0.028	0.214	0.325	0.211	0.009	
x_i	0.814	1.485	0.451	1.475	0.445	1.796	0.807	Step 2
$\hat{\lambda}_i$	0.187	0.249	0.308	0.249	0.312	0.356	0.187	
\hat{w}_i	0.286	0.278	0.117	0.0882	0.0628	0.004	0.141	
x_i	0.814	1.485	0.451	—	—	—	—	Step 3
$\hat{\lambda}_i$	0.187	0.249	0.308	—	—	—	—	
\hat{w}_i	0.426	0.369	0.183	—	—	—	—	

The whole numerical experiment and unfolding was repeated ten times. The number of obtained final components varied between three and six. The obtained p -values show no clear deviation from an evenly distribution between zero and unity, indicating that the measured distributions are typically reasonably well described by the folded estimates of the true distribution – supporting the validity of the unfolding approach.

3.2. Strongly varying one-sided distribution

In this example the above method is applied to unfold a strongly varying one-sided PDF. The true distribution, defined in the range $[0, +\infty)$, is

$$p(x) \propto x e^{-5x} . \quad (26)$$

Let us represent the true value x as a function of two variables u and v , $x = \sqrt{u^2 + v^2}$, with $u = x \cos(\phi)$ and $v = x \sin(\phi)$, with the angular variable ϕ uniformly distributed in $[0, 2\pi)$. The reconstructed value $x' = \sqrt{u'^2 + v'^2}$ is obtained from u' and v' , defined as independent random variables with normal distributions $\mathcal{N}(u, (0.5u)^2)$ and $\mathcal{N}(v, (0.5v)^2)$ respectively. Here we do not present an analytical formula for the resolution function $R(x'|x)$, but notice that it is a generalisation of the Rice distribution. An example for the measured distribution obtained by simulating a sample of $N = 10\,000$ events is presented in Fig. 7.

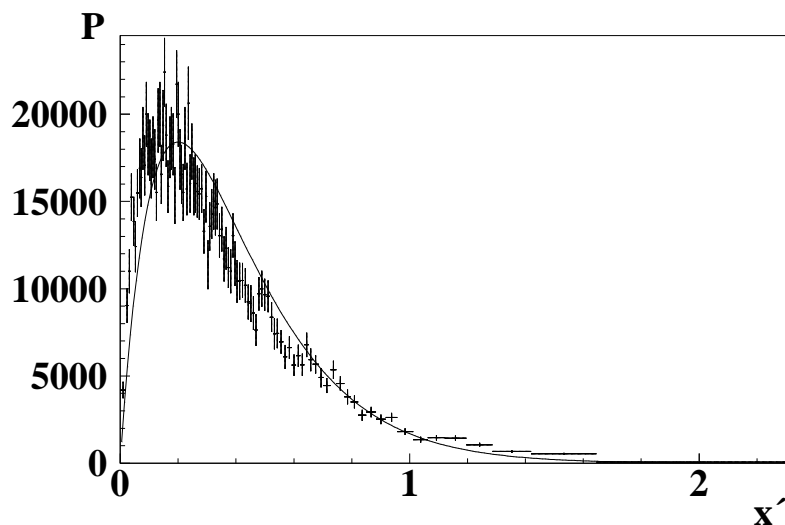


Figure 7: The histogram of the measured distribution \mathbf{P} based on a sample of 10 000 events generated for the true distribution. The true distribution $p(x)$ is shown by the curve.

In general the choice of PDFMs has should be adapted to the problem at hand, i.e. symmetric gaussian PDFMs as used in the previous example are not directly suitable for this kind of unfolding problem. The GMM fit

model can, however, be used after transforming the problem such that the true distribution becomes approximately gaussian in shape. The Box-Cox transformation [30]

$$x^{[\mu]} = \begin{cases} (x^\mu - 1)/\mu & \text{for } \mu \neq 0 \\ \ln x & \text{for } \mu = 0 \end{cases} \quad (27)$$

is appropriate for this case. After transforming the unfolding result back to the original variables, the entire procedure is equivalent to using a PDFMs of the form

$$K(x; x_i, \lambda, \mu) = \frac{1}{\lambda\sqrt{2\pi}} \exp\left(-\frac{(x^{[\mu]} - x_i^{[\mu]})^2}{2\lambda^2}\right) x^{(\mu-1)} . \quad (28)$$

For the determination of the matrix \mathbf{Q} a sample of 1 000 000 Monte Carlo events was simulated. The true distribution was taken to be uniform and the response of the PDFM was calculated by weighting the Monte Carlo events with weights proportional to the value of respective PDFMs [20]. In the first step an initial set of 400 PDFMs was used with positions x_i uniformly distributed over the interval $[0, 2]$. The transformation parameter $\mu = 0.25$ was used, which leads to a transformed PDF $P(x'^{[\mu]})$ with skewness close to 0.

As shown in Fig. 8, the constant width parameter $\hat{\lambda}_i = \hat{\lambda} = 0.5$ provides the minimum value for the Cross-Validation error $CV(\lambda)$. In the second step $\hat{\lambda}_i$ is not constant but inversely proportional to the square root of the unfolded density obtained in the first step in order to have better smoothing in regions of low statistics. Here one finds a preferred value of $\hat{\lambda} = 0.39$. In this case the Cross-Validation error does not improve. In the third step finally a best value for the garrote parameter $r = 2.8$ is found for $\hat{\lambda} = 0.39$. The minimum, however, is not very pronounced. These two parameters are used for the final calculation of the unfolded distribution. Only three terms are retained for the estimate of the true distribution.

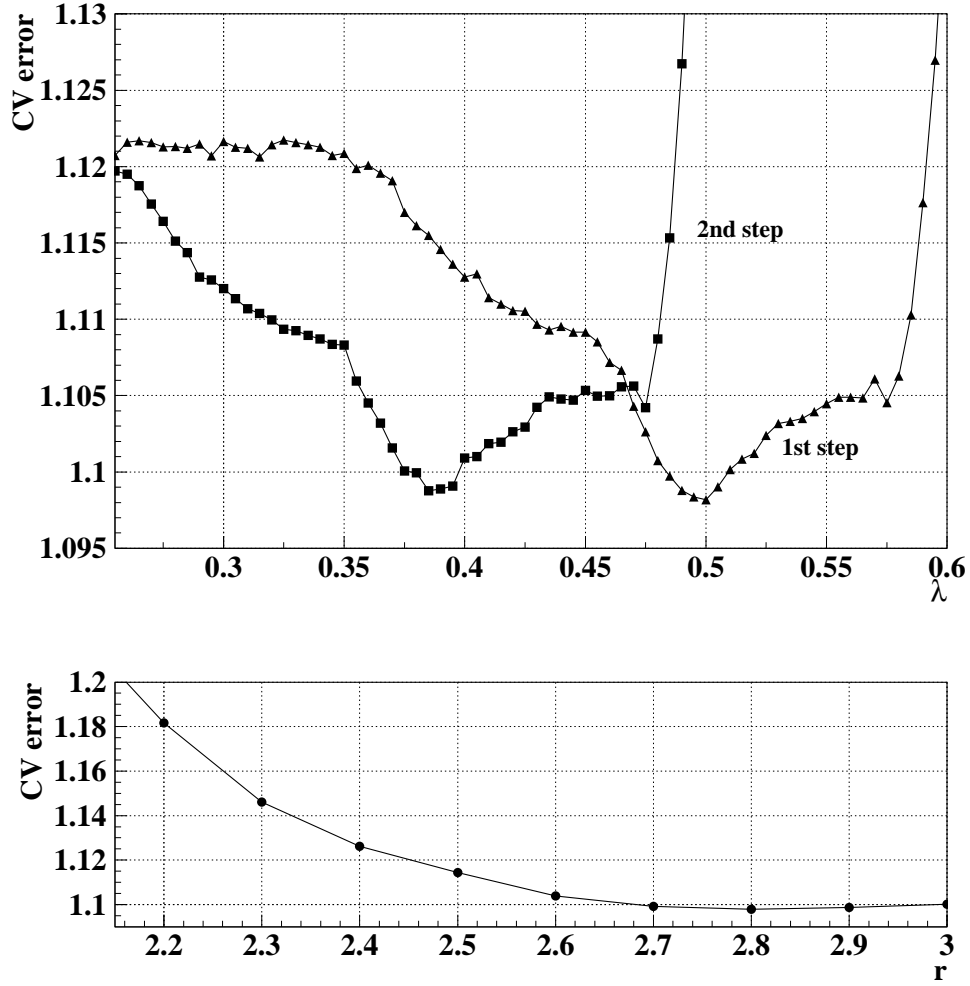


Figure 8: Cross-Validation errors for different values of λ (top) and Cross-Validation errors for different values of r ($\lambda = 0.39$) (bottom).

Figure 9 illustrates the quality of the fit. No structure in either of the control plots is observed. The p -value from the test for the comparison of the histogram of the measured distribution \mathbf{P} and the fitting histogram $\hat{\mathbf{P}}$, Fig. 9(a), is $p = 0.43$. The components of the unfolding results are shown together with the estimate $\hat{p}(x)$ in Fig. 10. Also shown are the standard deviation bands $\pm 2\delta(x)$ compared to the true distribution $p(x)$. The binned presentation of the unfolded distribution shown in Fig. 11 was done with $n = 21$ bins.

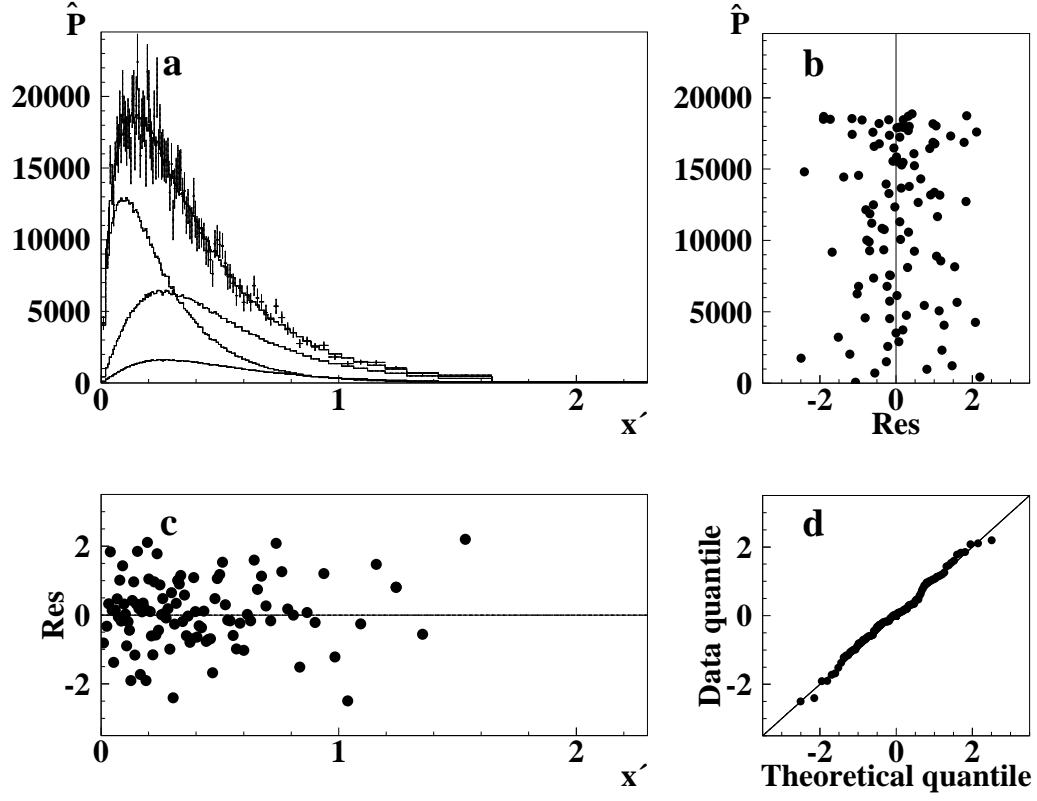


Figure 9: Illustration of the quality of the unfolding result: (a) folded estimate of the true distribution \hat{P} (solid histogram) compared to the measured distribution P ; (b) normalised residuals of the fit as a function of \hat{P} ; (c) normalised residuals as a function of x' ; (d) quantile-quantile-plot for the normalised residuals.

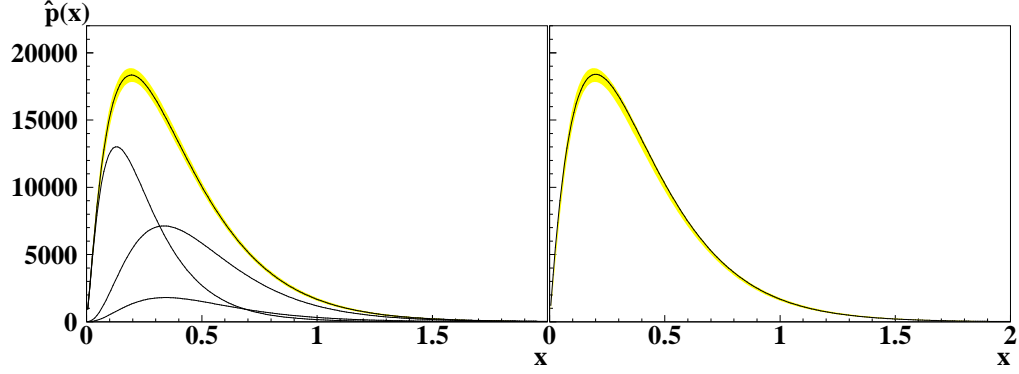


Figure 10: Components of the unfolded distribution and the unfolded distribution $\hat{p}(x)$ given by the sum of the components with $\pm 2\delta(x)$ interval (left) and the two standard deviations band overlaid with the true distribution $p(x)$ (right).

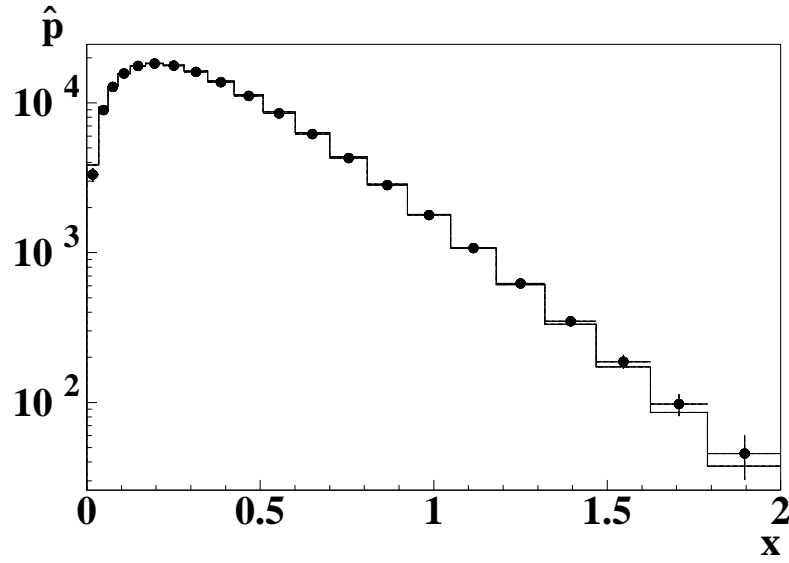


Figure 11: Binned representation of the unfolding results \hat{p}_i for $m = 21$ bins. The vertical error bars denote the standard deviations δ_i . The histogram shows the true bin contents p_i .

3.3. Two-dimensional unfolding

The method presented in this paper is also directly applicable to multidimensional cases. Here a two-dimensional example is given. The true distribution defined on the two-dimensional domain $x, y \in [10, 40] \times [10, 40]$ and represented by a sum of three bivariate gaussian PDFs $p_g(x, y; \mu_x, \mu_y, \sigma_x, \sigma_y, \rho)$, with μ_x, μ_y the expectation values, σ_x, σ_y the standard deviations and ρ the correlations coefficient. The actual density is given by

$$\begin{aligned} p(x, y) \propto & 4 p_g(x, y; 20.5, 25.5, 4.0, 4.0, 0.5) \\ & + p_g(x, y; 30.5, 25.5, 3.0, 3.0, 0.0) \\ & + 5 p_g(x, y; 35.0, 23.0, 20.0, 30.0, 0.0) . \end{aligned} \quad (29)$$

The experimentally measured distribution is obtained by

$$P(x', y') \propto \int_{10}^{40} \int_{10}^{40} p(x, y) R(x', y' | x, y) dx dy , \quad (30)$$

with a resolution function

$$\begin{aligned} R(x', y' | x, y) \propto & p_g(x', y'; x, y, 1.0, 1.0, 0.0) \\ & + 0.5 p_g(x', y'; x, y, 2.5, 2.5, 0.0) \\ & + 0.05 p_g(x', y'; x, y, 5.0, 5.0, 0.0) . \end{aligned} \quad (31)$$

An example of a measured distribution is obtained by simulating a sample of $N = 10\,000$ events. In Figure 12 the true density and the measured distribution are shown. While the dominant component (first gaussian) is still clearly visible in the observed distribution, the weak component (second gaussian) is barely discernible.

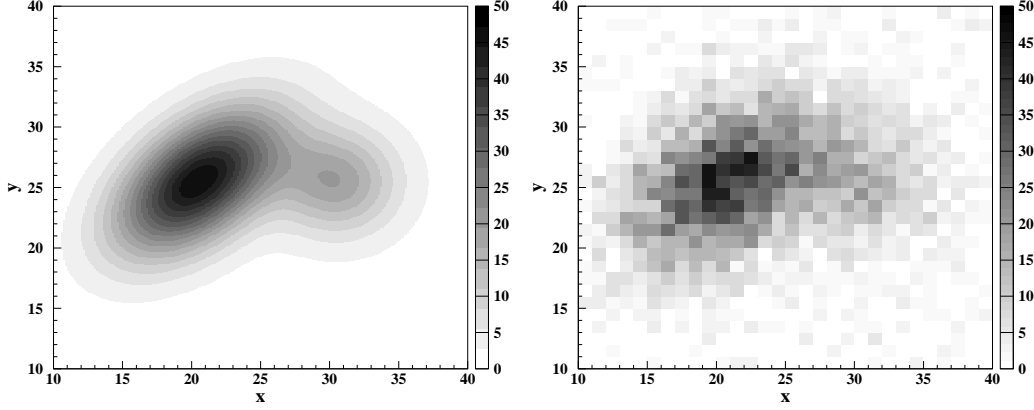


Figure 12: The true distribution $p(x, y)$ (left) and histogram of the measured distribution \mathbf{P} based on a sample of 10 000 events (right).

To use the existing software, a one-dimensional histogram was created from the two-dimensional distribution by copying first the top row from left to right then the 2nd row from right to left and so on. Adjacent bins of the one-dimensional histogram with a low number of events were merged to have at least 25 events per bin. The vector of the histogram contents \mathbf{P} finally used in the unfolding procedure has $n = 196$ components. For the determination of the matrix \mathbf{Q} a sample of 1 000 000 Monte Carlo events was simulated. PDFMs were defined as circular symmetric gaussian probability density functions with three parameters, the expectation values x_i, y_i and the standard deviation λ_i . In the first step, a set of 400 PDFMs was used with positions x_i, y_i uniformly distributed over the domain $x, y \in [10, 40] \times [10, 40]$. As shown in Fig. 13, using 5-fold Cross-Validation, an optimal value $\hat{\lambda}_i = \hat{\lambda} = 3.0$ is found. For the second step, with an adaptive width $\hat{\lambda}_i$ inversely proportional to the square root of the unfolded density obtained in the first step, the value $\hat{\lambda} = 0.16$ minimises the Cross-Validation error $CV(\lambda)$. In the third step the optimal garrote parameter for $\hat{\lambda} = 0.16$ is found to be $r = 21.2$. These two parameters are used for the final calculation of the unfolded distribution.

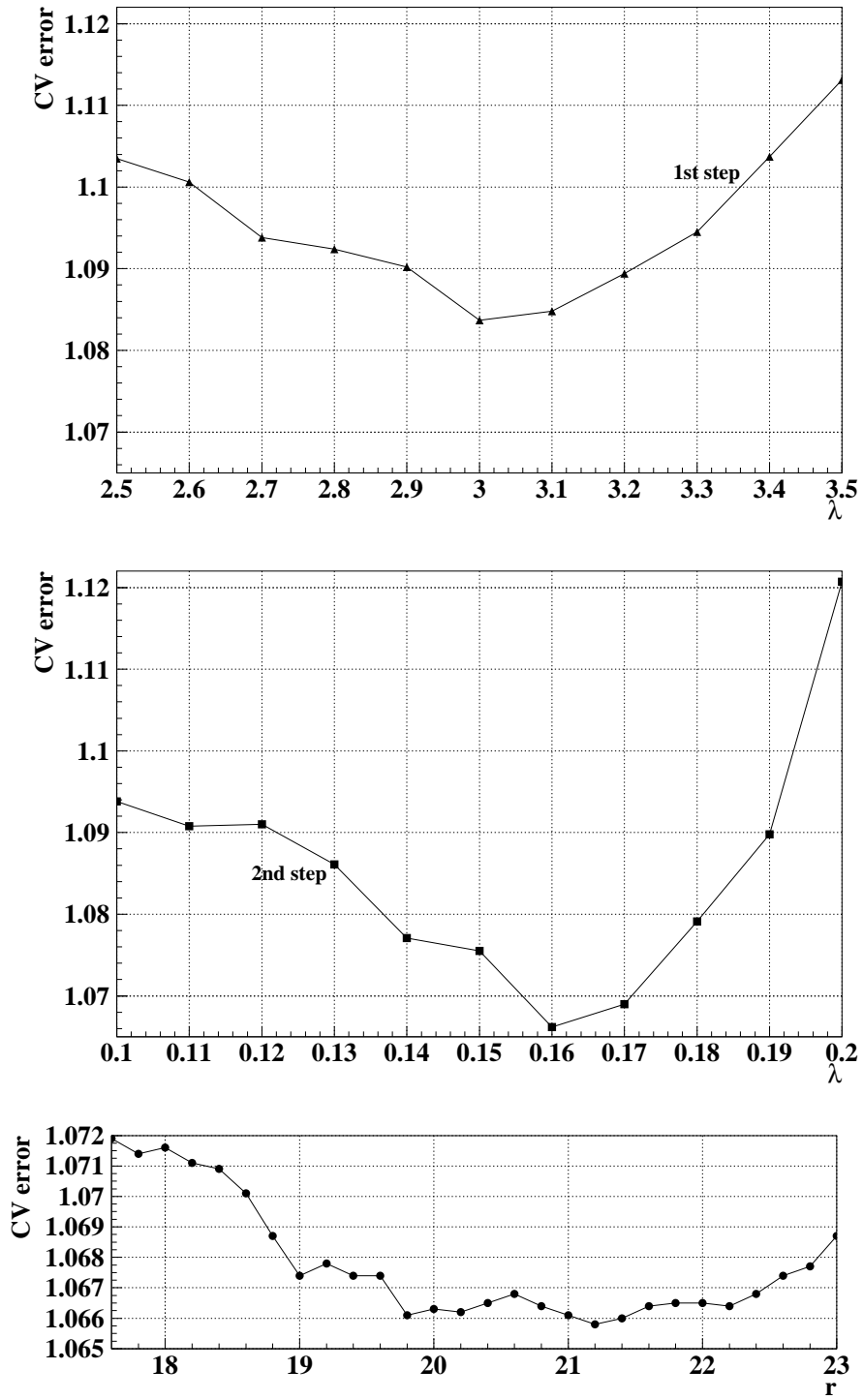


Figure 13: Cross-Validation as a function of λ in step 1 (top) and step 2 (middle), and as a function of the garrote parameter r for $\lambda = 0.16$ from the second step (bottom).

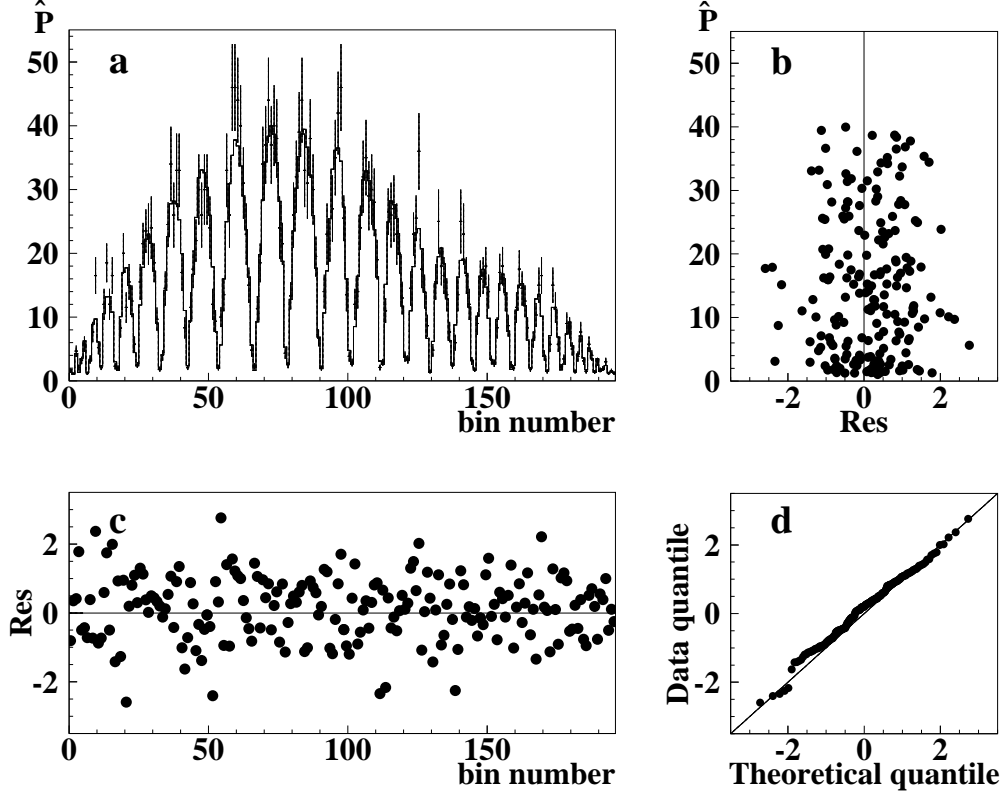


Figure 14: Illustration of the quality of the unfolding result. (a) folded estimate of the true distribution $\hat{\mathbf{P}}$ (solid histogram) compared to the measured distribution \mathbf{P} ; (b) normalised residuals of the fit as a function of $\hat{\mathbf{P}}$; (c) normalised residuals as a function of bin number; (d) quantile-quantile plot for the normalised residuals.

The quality of the unfolding result is illustrated by Fig. 14. It shows the mixture of the folded gaussian PDFMs, which approximates the measured distribution, together with the analysis of the residual and the quantile-quantile plot. No structure in either of the control plots is observed. The p -value for the comparison of the histogram of the measured distribution \mathbf{P} and the fitting histogram $\hat{\mathbf{P}}$ is $p = 0.19$.

The unfolded distribution $\hat{p}(x, y)$ is presented in Fig. 15 together with the difference between the unfolded and the true distribution $\hat{p}(x, y) - p(x, y)$. One observes that the true distribution, including its weak component, is

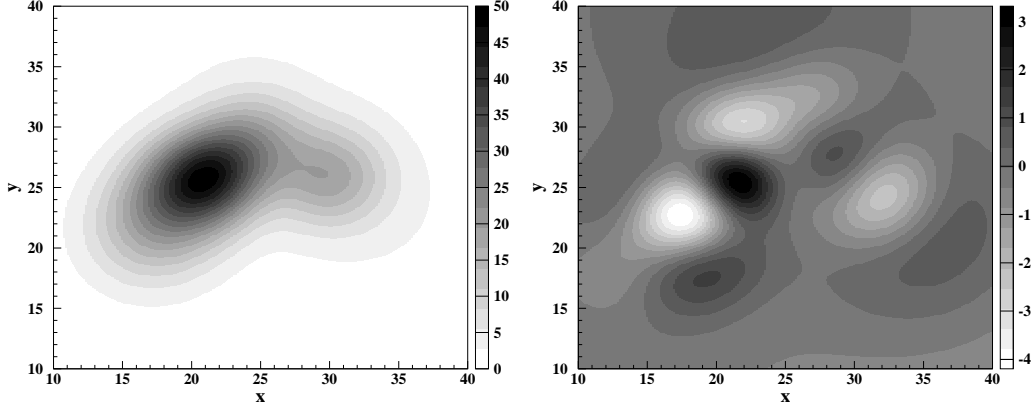


Figure 15: The unfolded distribution $\hat{p}(x, y)$ (left) and the difference between unfolded and true distribution $\hat{p}(x, y) - p(x, y)$ (right).

well reproduced by the unfolding result, with rather small deviations of the unfolded distribution from the true one.

4. Summary and conclusions

A new method for unfolding the true distribution from data obtained from detectors with finite resolution and limited acceptance is presented. The method ensures smoothness and positivity of the result by representing the true distribution as a weighted sum of smooth PDFs (Mixture Densities Model). The standard deviation of the PDFs acts as a regularisation parameter which determines the smoothness of the result. The amount of smoothing is adjusted to the local statistical precision of the data by scaling the width parameter inversely proportional to square root of the estimated density and the non-negative garrote method is used to eliminate insignificant terms in the solution. Cross-Validation is used to determine optimal values of the regularisation and garrote parameters. The method avoids discretisation of the true density entering the integral equation, thereby avoiding quantisation errors for the true distribution. The proposed procedure is directly applicable to multidimensional unfolding problems. Numerical examples covering

the problems of unfolding a simple double-peak structure, a strongly varying one-side distribution and a two-dimensional density were presented to illustrate and to validate the procedure

Acknowledgements

The author would like to express very great appreciation to Michael Schmelling for constant interest to this work and many discussions stimulating the development of the method. The author is also grateful to Markward Britsch for useful discussions as well as for careful reading of the manuscript. Special thanks are extended to the University of Akureyri and the MPI for Nuclear Physics for support in carrying out the research.

References

- [1] N. D. Gagunashvili, Nucl. Instr. Meth. A 635 (2011) 86.
- [2] V. V. Ammosov, Z. U. Usubov, V. P. Zhigunov, Nucl. Instr. Meth. A 295 (1990) 224.
- [3] G. Bohm, G. Zech, Introduction to Statistics and Data Analysis for Physicists, ch. 6, Verlag Deutsches Elektronen-Synchrotron, 2010.
- [4] V. P. Zhigunov, Nucl. Instr. Meth. 216 (1983) 183.
- [5] V. Blobel, CERN 85-02, 1985.
- [6] V. B. Anikeev, A. A. Spiridonov, V. P. Zhigunov, Nucl. Instr. Meth. A 322 (1992) 280.
- [7] N. Gagunashvili, Nucl. Instr. Meth. A 343 (1993) 606.
- [8] M. Schmelling, Nucl. Instr. Meth. A 340 (1994) 400.
- [9] A. Höcker, V. Kartvelishvili, Nucl. Instr. Meth. A 372 (1996) 469.
- [10] L. Lindemann, G. Zech, Nucl. Instr. Meth. A 354 (1995) 516.
- [11] G. D'Agostini, Nucl. Instr. Meth. A 362 (1995) 487.

- [12] V. Blobel, An unfolding method for high-energy physics experiments, in: Proceedings of the Conference on Statistical Problems in Particle Physics, Durham, England, 18–22 March 2002, 258–267.
- [13] N. Gagunashvili, Unfolding with system identification, in: Proceedings of the Conference on Statistical Problems in Particle Physics, Astrophysics and Cosmology, 12–15 September, 2005, Oxford, Imperial College Press, London, 2006, pp. 267–210.
- [14] J. Albert et al., Nucl. Instr. Meth. A 583 (2007) 494.
- [15] B. W. Silverman, Density Estimations for Statistics and Data Analysis, Chapman and Hall, 1986.
- [16] M. L. Hazelton, B. A. Turlach, Stat. Comput. 19 (2009) 217.
- [17] G. McLachlan, ed.: Mixture Models. Marcel Dekker, 1988.
- [18] D. Reynolds, Gaussian Mixture Models, in: Encyclopedia of Biometrics, pp 659–663, Springer, 2009.
- [19] C. R. Shalizi, Advanced Data Analysis from an Elementary Point of View, ch.19, <http://www.stat.cmu.edu/~cshalizi/ADAfaEPoV/>, 2013.
- [20] I. M. Sobol, Numerical Monte Carlo Methods, ch. 5, Nauka, Moscow, 1973.
- [21] C. L. Lawson and R. J. Hanson, Solving Least Squares Problems, ch. 23, sec. 3, Prentice-Hall, Englewood Cliffs, 1974; also available as Classics in Applied Mathematics, Vol. 15, SIAM, Philadelphia, 1995.
- [22] <http://www.netlib.org/lawson-hanson/all>, subroutine NNLS.
- [23] L. Breiman, Technometrics, 37 (1995) 373.
- [24] I. S. Abramson, Annals of Statistics, 10 (1982) 1217.
- [25] G. A. F. Seber and A. J. Lee, Linear Regression Analysis, John Wiley & Sons, 2003.
- [26] B. Efron, Annals of Statistics, 7 (1979) 1.
- [27] V. V. Fedorov, Biometrika, 61 (1974) 49.

- [28] N. D. Gagunashvili, Nucl. Instr. Meth. A 614 (2010) 287.
- [29] N. D. Gagunashvili, Comp. Phys. Comm. 183 (2012) 193.
- [30] R. M. Sakia, The Statistician, 41 (1992) 169.